Initial state characteristics of proton-nucleus collisions from Glauber Monte Carlo*

Maciej Rybczyński and Zbigniew Włodarczyk
Jan Kochanowski University, Kielce, Poland

*based on M. Rybczyński, Acta. Phys. Pol. B45 (2014) 89

GLISSANDO

GLauber Initial State Simulation AND mOre

www.ujk.edu.pl/homepages/mryb/GLISSANDO/

GLISSANDO is a Glauber Monte-Carlo generator for early-stages of relativistic heavy-ion collisions, written in c++ and interfaced to ROOT.

The program can be used for simulation of large variety of colliding systems: p+A, d+A and A+A at wide spectrum of energies.

Several models are implemented: the wounded-nucleon model, the binary collisions model, the mixed model, and the model with hot-spots.

Nuclear correlations –

why nucleon-nucleon expulsion distance should be d=0.9 fm?

Alvioli, Drescher and Strikman generated distributions of nucleons in nuclei which account for the central two-body **nucleon-nucleon correlations**.
The procedure, based on the Metropolis search for configurations satisfying constrains imposed by the **nucleon-nucleon correlations**, reproduces the one-body Woods-Saxon distributions as well as central nucleon-nucleon correlations, taken in the Gaussian form.

M. Alvioli, H.J Drescher and M. Strikman, Phys. Lett. B680, 225
http://www.phys.psu.edu/~malvioli/eventgenerator/

$$C(r) = 1 - \frac{\rho_C^{(2)}(r)}{\rho_U^{(2)}(r)}$$

$$\rho_C^{(2)}(r) = \int d^2\Omega \int d^3R \rho^{(2)}(\boldsymbol{R}+\boldsymbol{r}/2, \boldsymbol{R}-\boldsymbol{r}/2)$$
$$\rho_U^{(2)}(r) = \int d^2\Omega \int d^3R \rho^{(1)}(\boldsymbol{R}+\boldsymbol{r}/2, \boldsymbol{R}-\boldsymbol{r}/2) \cdot \rho^{(1)}(\boldsymbol{R}+\boldsymbol{r}/2, \boldsymbol{R}-\boldsymbol{r}/2)$$

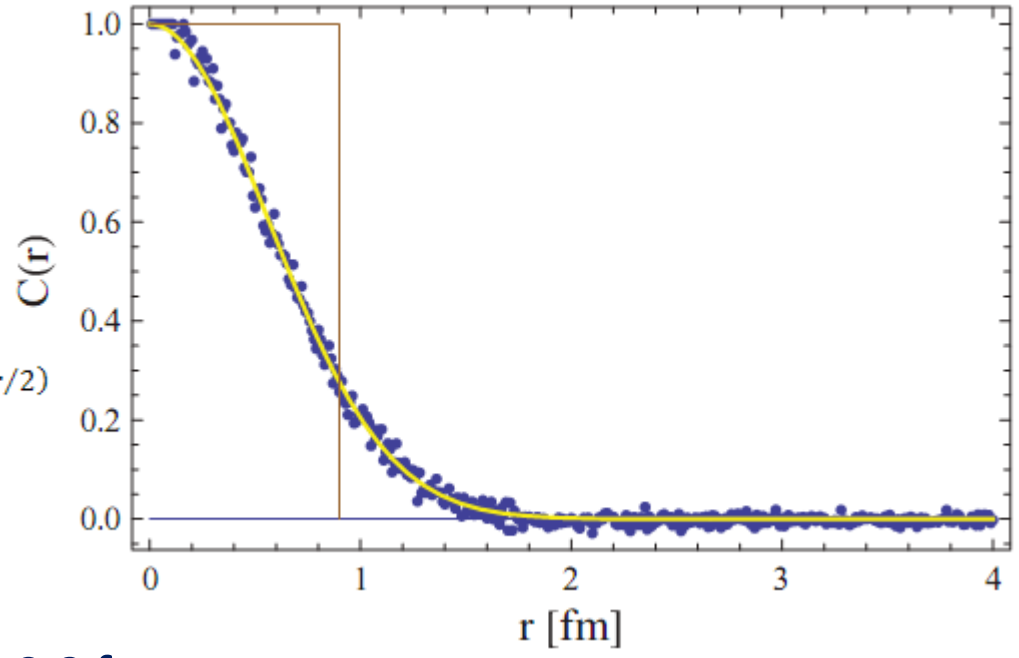

The effects of these correlations on heavy-ion observables turn out to be indistinguishable from the hard-core repulsion with d=0.9 fm

Details in:
W. Broniowski, M. Rybczynski, Phys. Rev. C81 (2010) 064909

The nucleon-nucleon wounding profile

The nucleon-nucleon wounding profile, $p\,(b)$ is normalized to *the total inelastic nucleon-nucleon cross section,* σ^{inel}

$$2\pi \int bp(b)db = \sigma^{inel}$$

1) **hard-sphere approximation:**

$$p_{HS}(b) = \theta\left(\sqrt{\sigma^{inel}/\pi} - b\right)$$

2) **Gaussian approximation:**

$$p_G(b) = A\exp\left(-\frac{\pi A b^2}{\sigma^{inel}}\right)$$

3) **gamma approximation:**

$$p_\Gamma(b) = \mathrm{G}\Gamma\left(\frac{1}{\omega}, \frac{\pi G b^2}{\sigma^{inel}\omega}\right)\Big/\Gamma\left(\frac{1}{\omega}\right)$$

$$\lim_{\omega\to 0} p_\Gamma(b) = p_{HS}(b)$$

$$\lim_{\omega\to 1} p_\Gamma(b) = p_G(b)$$

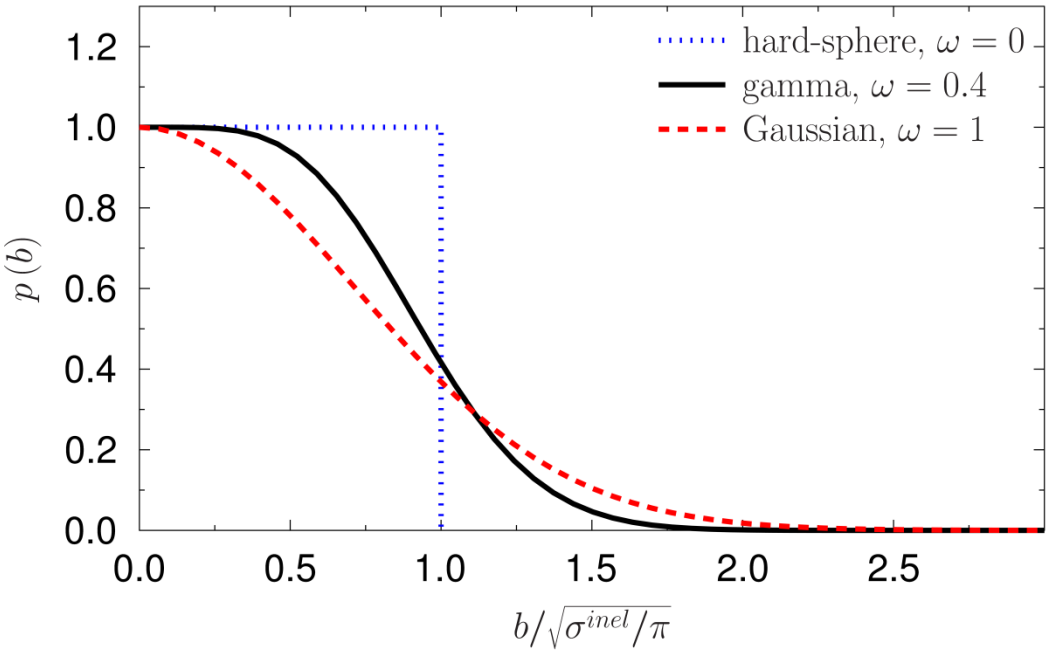

Gaussian wounding profile explains the nucleon-nucleon elastic differential cross section at ISR
(Białas and Bzdak, Acta Phys. Polon. B38, 159)

Details in:
M. Rybczyński, Z. Włodarczyk, J. Phys. G41 (2014) 015106

The nucleon-nucleon wounding profile

$$\omega_p^{targ} = \frac{\mathrm{Var}\left(N_p^{targ}\right)}{\langle N_p^{targ} \rangle}$$

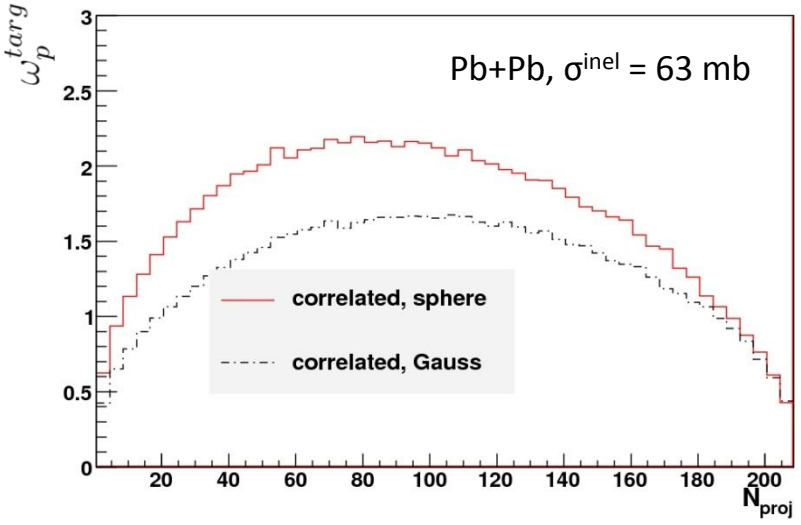

$$\varepsilon^* = \frac{\sqrt{\left(\sigma_y^2 - \sigma_x^2\right)^2 + 4\sigma_{xy}^2}}{\sigma_y^2 + \sigma_x^2}$$

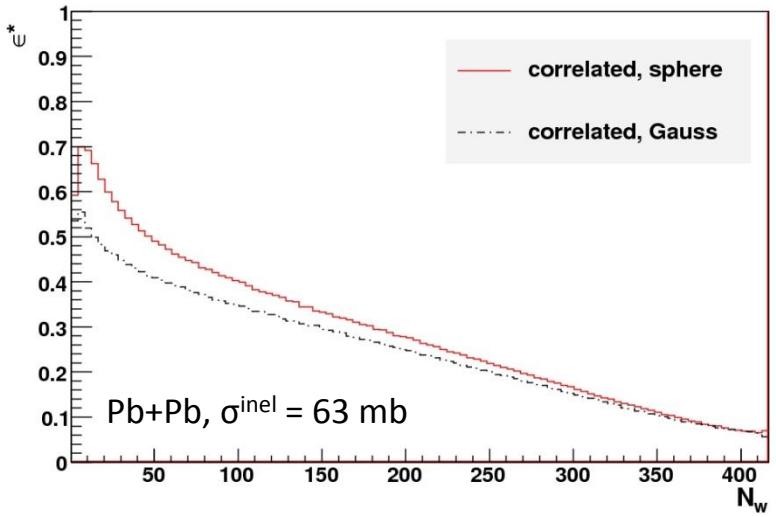

Nuclear density

For nuclei with A > 16
deformed Woods-Saxon density:

$$\rho(r) = \frac{\rho_0}{1 + \exp\left(\frac{r - R(1 + \beta_2 Y_{20} + \beta_4 Y_{40})}{a}\right)}$$

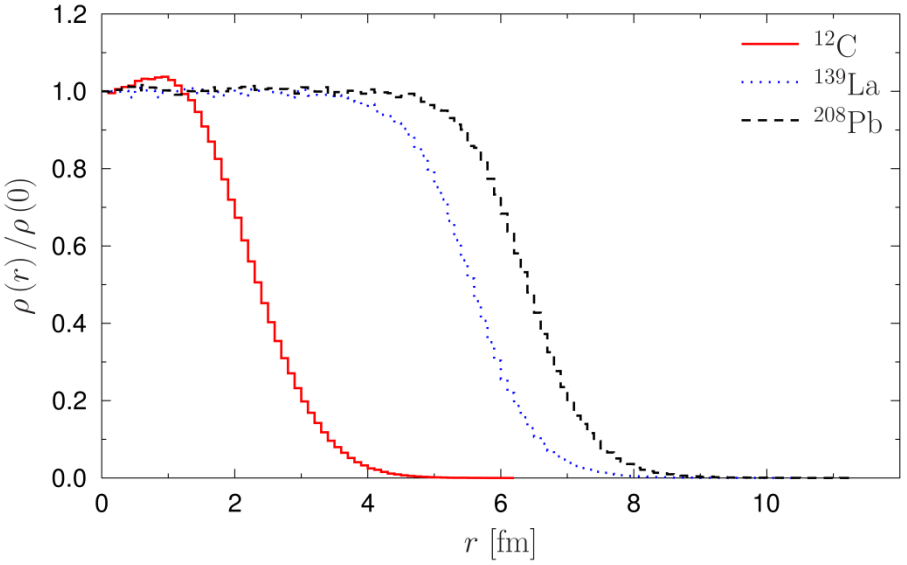

For nuclei with 3 ≤ A ≤ 16
harmonic oscillator shell model density:

$$\rho(r) = \frac{4}{\pi^{3/2} C^3}\left[1 + \frac{A-4}{6}\left(\frac{r}{C}\right)^2\right]\exp\left(-\frac{r^2}{C^2}\right)$$

$$C^2 = \left(\frac{5}{2} - \frac{4}{A}\right)^{-1}\left(\langle r_{ch}^2\rangle_A - \langle r_{ch}^2\rangle_p\right)$$

Atomic Data And Nuclear Data Tables 36, 495
Atomic Data And Nuclear Data Tables 99, 69

Nuclear density parameters

For nuclei with A > 16:

deformed Woods-Saxon density:

$d = 0$

$$R = \left(1.12A^{1/3} - 0.86A^{-1/3}\right) \text{ fm}$$

$$a = 0.54 \text{ fm}$$

$d = 0.9$ fm

$$R = \left(1.1A^{1/3} - 0.656A^{-1/3}\right) \text{ fm}$$

$$a = 0.459 \text{ fm}$$

Nuclear density parameters

For nuclei with A > 16:

deformed Woods-Saxon density:

$$d = 0$$

$$R = \left(1.12A^{1/3} - 0.86A^{-1/3}\right) \text{ fm}$$

$$a = 0.54 \text{ fm}$$

$$d = 0.9 \text{ fm}$$

$$R = \left(1.1A^{1/3} - 0.656A^{-1/3}\right) \text{ fm}$$

$$a = 0.459 \text{ fm}$$

Nucleus	R [fm]	β_2	β_4
^{40}Ar	3.57	0.0	0.0
^{40}Ca	3.57	0.0	0.0
^{45}Sc	3.73	0.0	0.0
^{63}Cu	4.21	1.162	-0.006
^{129}Xe	5.43	0.143	-0.001
^{139}La	5.57	0.0	0.0
^{208}Pb	6.41	0.0	0.0

Nuclear density parameters

For nuclei with A > 16:

deformed Woods-Saxon density:

$$d = 0$$
$$R = \left(1.12A^{1/3} - 0.86A^{-1/3}\right) \text{ fm}$$
$$a = 0.54 \text{ fm}$$

$$d = 0.9 \text{ fm}$$
$$R = \left(1.1A^{1/3} - 0.656A^{-1/3}\right) \text{ fm}$$
$$a = 0.459 \text{ fm}$$

Nucleus	R [fm]	β_2	β_4
^{40}Ar	3.57	0.0	0.0
^{40}Ca	3.57	0.0	0.0
^{45}Sc	3.73	0.0	0.0
^{63}Cu	4.21	1.162	-0.006
^{129}Xe	5.43	0.143	-0.001
^{139}La	5.57	0.0	0.0
^{208}Pb	6.41	0.0	0.0

For nuclei with 3 ≤ A ≤ 16:

harmonic oscillator shell model density:

Nucleus	$\langle r_{ch}^2 \rangle_A$ [fm^2]	
	$d = 0$	$d = 0.9$ fm
^{7}Be	7.00	6.69
^{9}Be	6.35	6.00
^{12}C	6.10	5.66
^{14}N	6.54	6.08
^{16}O	7.29	6.81

Atomic Data and Nuclear Data Tables 36, 495
Atomic Data and Nuclear Data Tables 59, 185
Atomic Data And Nuclear Data Tables 99 , 69

Results:

The following reactions were studied:

$p + {}^{12}C$
$p + {}^{14}N$
$p + {}^{63}Cu$
$p + {}^{208}Pb$

The used total inelastic proton-proton cross sections, σ^{inel}
for different nucleon-nucleon centre-of-mass eneries, $\sqrt{s}$ (momenta in lab frame, p_{lab}):

$\sqrt{s}$ [GeV]	p_{lab} [GeV/c]	σ^{inel} [mb]
5.12	13.0	29.1
16.83	150.0	31.72
7000.0	$2.6\ 10^7$	73.5

J. Beringer *et al. [Particle Data Group Collaboration], Phys. Rev. D 86*, 010001

Results:
mean number of target participants

$$\langle N_p^{targ} \rangle = N_o A^{\alpha}$$

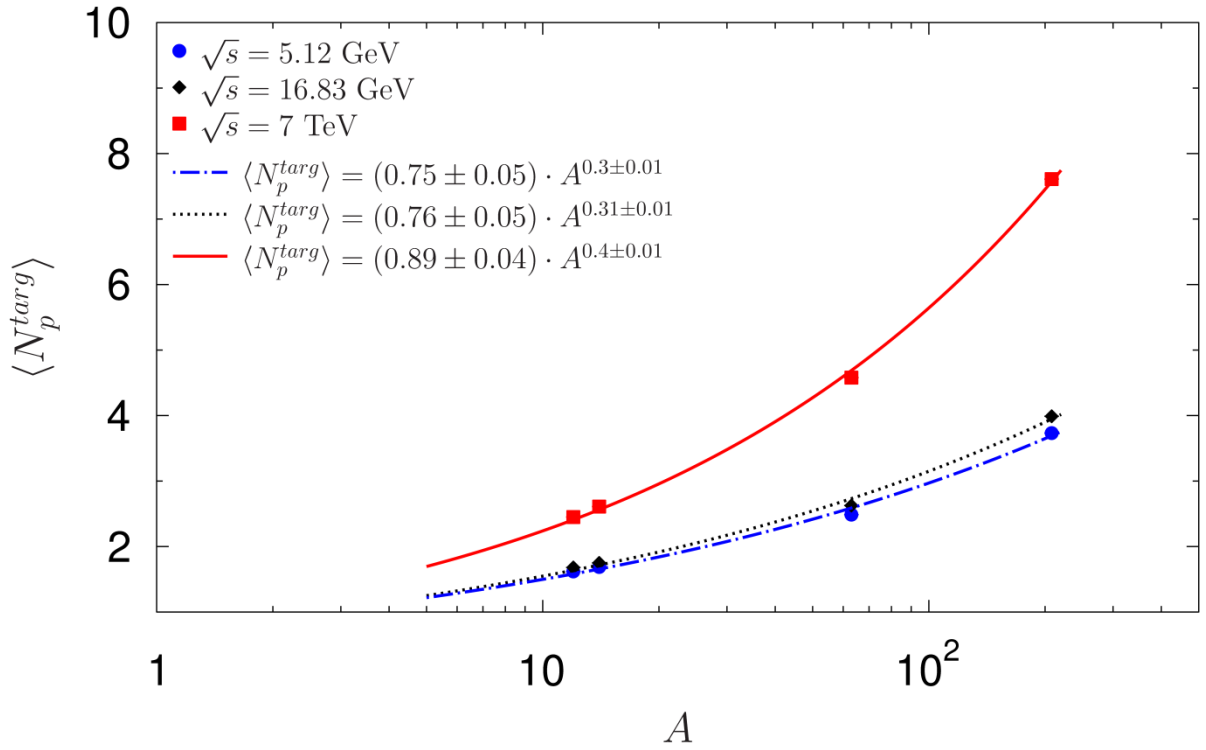

$\sqrt{s}$ [GeV]	N_0	α
5.12	0.75 ± 0.05	0.3 ± 0.01
16.83	0.76 ± 0.05	0.31 ± 0.01
7000.0	0.89 ± 0.04	0.4 ± 0.01

Nucleon-nucleon wounding profile given by hard-sphere approximation

Results:
fluctuations of the number of target participants

$$\omega_p^{targ} = \frac{\mathrm{Var}\left(N_p^{targ}\right)}{\langle N_p^{targ} \rangle}$$

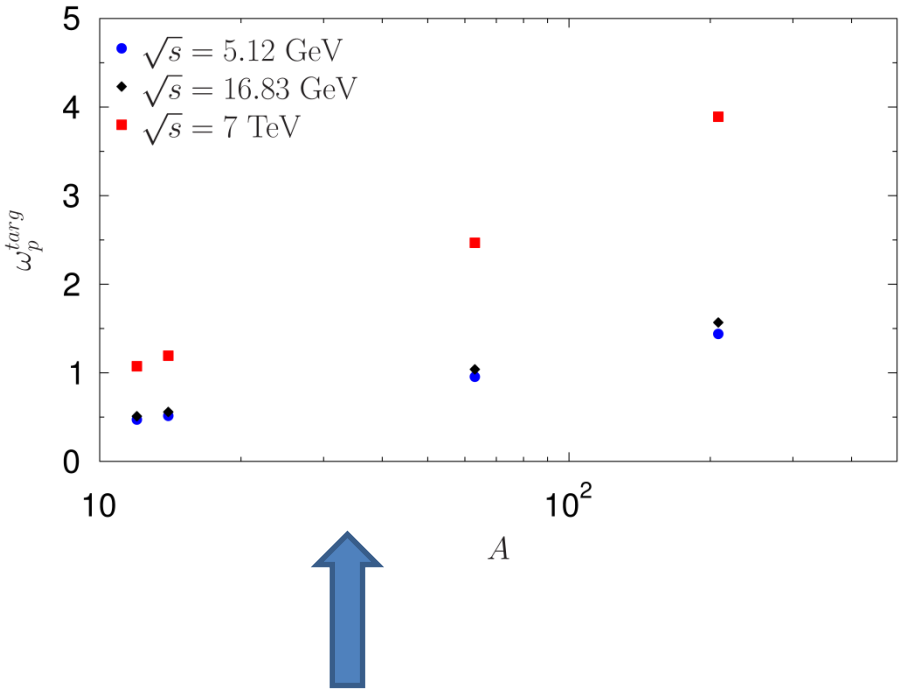

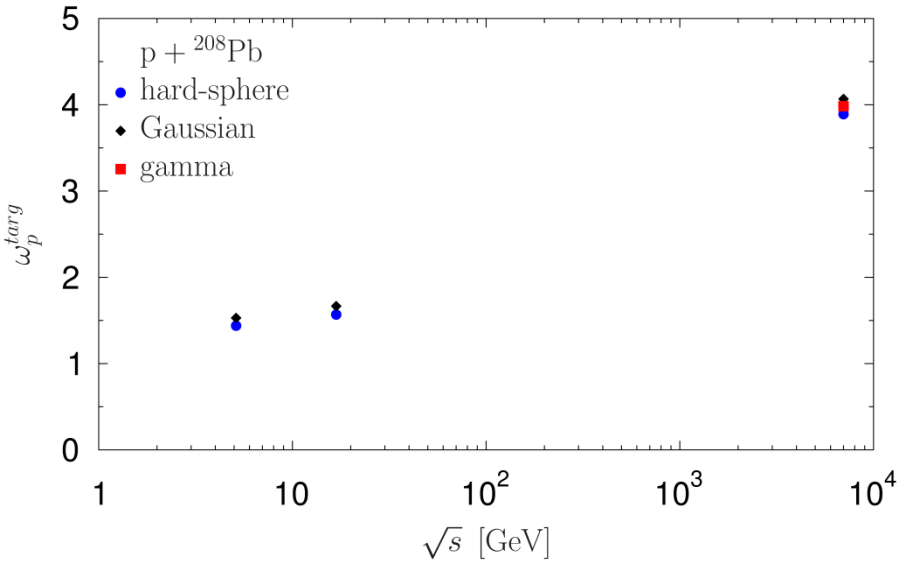

Nucleon-nucleon wounding profile
given by hard-sphere approximation

Results:
production cross section

The production processes are those
which lead to production of new hadrons.
For the simulation of production processes,
the total inelastic proton–proton cross section
was applied.

Results:
production cross section

The production processes are those which lead to production of new hadrons. For the simulation of production processes, the total inelastic proton–proton cross section was applied.

Production cross section, σ_{p+N}^{prod}, for $p + {}^{14}N$ interactions at $\sqrt{s} = 7000$ GeV.
Simulation performed with total inelastic proton–proton cross section $\sigma^{inel} = 73.5^{+1.8}_{-1.3}$ mb.
The upper (positive) uncertainty comes from simulations with $\sigma^{inel} = 75.3$ mb while the lower one — from $\sigma^{inel} = 72.2$ mb.

$d\ [fm]$	$\sigma_{p+N}^{prod}\ [mb]$ $(hard-sphere)$	$\sigma_{p+N}^{prod}\ [mb]$ $(gamma)$	$\sigma_{p+N}^{prod}\ [mb]$ $(Gaussian)$
0	$391.5^{+5.1}_{-3.7}$	$413.7^{+5.6}_{-4.2}$	$451.7^{+7.5}_{-5.1}$
0.9	$394.3^{+5.1}_{-3.3}$	$415.1^{+6.0}_{-4.1}$	$452.4^{+7.4}_{-5.5}$
1.5	$396.7^{+4.9}_{-3.4}$	$416.3^{+5.9}_{-3.6}$	$452.3^{+6.9}_{-5.3}$

Results:
production cross section

The production processes are those which lead to production of new hadrons. For the simulation of production processes, the total inelastic proton–proton cross section was applied.

$$\sigma_{p+A}^{prod} = \sigma_o A^{\gamma}$$

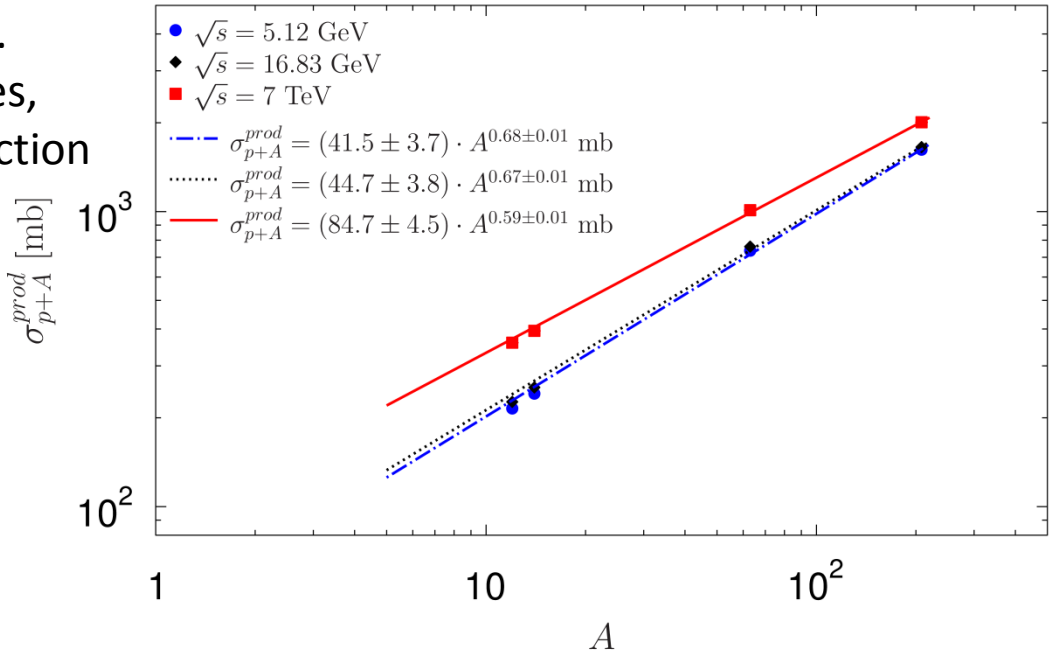

$\sqrt{s}$ [GeV]	σ_0 [mb]	γ
5.12	41.5 ± 3.7	0.68 ± 0.01
16.83	44.7 ± 3.8	0.67 ± 0.01
7000.0	84.7 ± 4.5	0.59 ± 0.01

Nucleon-nucleon wounding profile given by hard-sphere approximation

Results:
production cross section

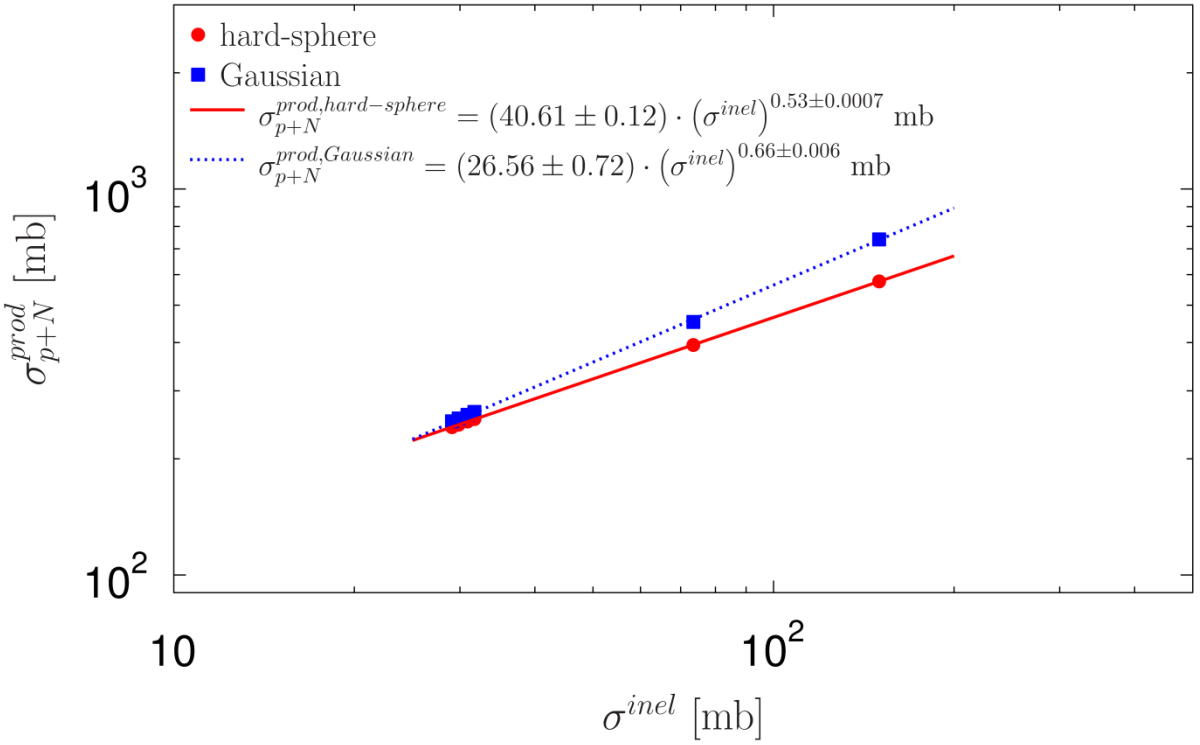

$$\sigma_{p+N}^{prod,hard-sphere} = (40.61 \pm 0.12)\left(\sigma^{inel}\right)^{0.53\pm0.0007} \text{ [mb]} \quad (*)$$

$$\sigma_{p+N}^{prod,Gaussian} = (26.56 \pm 0.72)\left(\sigma^{inel}\right)^{0.66\pm0.006} \text{ [mb]} \quad (**)$$

Results:
production cross section

Recently, the Pierre Auger Collaboration calculated the proton–air production cross section, σ_{p+air}^{prod} at $\sqrt{s} = 57\ \mathrm{TeV}$ from cosmic ray data, to be equal $\sigma_{p+air}^{prod} = 505^{+28}_{-36}\ \mathrm{mb}$.

There was also found the corresponding inelastic proton–proton cross section, $\sigma^{inel} = 92^{+9}_{-11}\ \mathrm{mb}$

Pierre Auger Collaboration data from:
P. Abreu et al. [Pierre Auger Collaboration], Phys. Rev. Lett. 109 (2012) 062002 [arXiv:1208.1520 [hep-ex]].

Results:
production cross section

Recently, the Pierre Auger Collaboration calculated the proton–air production cross section, σ_{p+air}^{prod} at $\sqrt{s} = 57\ \mathrm{TeV}$ from cosmic ray data, to be equal $\sigma_{p+air}^{prod} = 505^{+28}_{-36}\ \mathrm{mb}$.

There was also found the corresponding inelastic proton–proton cross section, $\sigma^{inel} = 92^{+9}_{-11}\ \mathrm{mb}$

From our fits (*) and (**) to $p + {}^{14}N$ GLISSANDO simulation, we found

$$\sigma_{p+N}^{prod,\ hard-sphere}(92\ \mathrm{mb}) = 446\ \mathrm{mb}$$

and

$$\sigma_{p+N}^{prod,\ Gaussian}(92\ \mathrm{mb}) = 525\ \mathrm{mb}$$

what determines the limits for production cross section at $\sqrt{s} = 57\ \mathrm{TeV}$ and is in quite good agrement with Pierre Auger Collaboration results.

Pierre Auger Collaboration data from:
P. Abreu et al. [Pierre Auger Collaboration], Phys. Rev. Lett. 109 (2012) 062002 [arXiv:1208.1520 [hep-ex]].

Results:

Recently,
cross sect

There wa

From our

$\sigma_{p+N}^{prod,\ h}$

and

$\sigma_{p+N}^{prod,\ G}$

what dete
and is in c

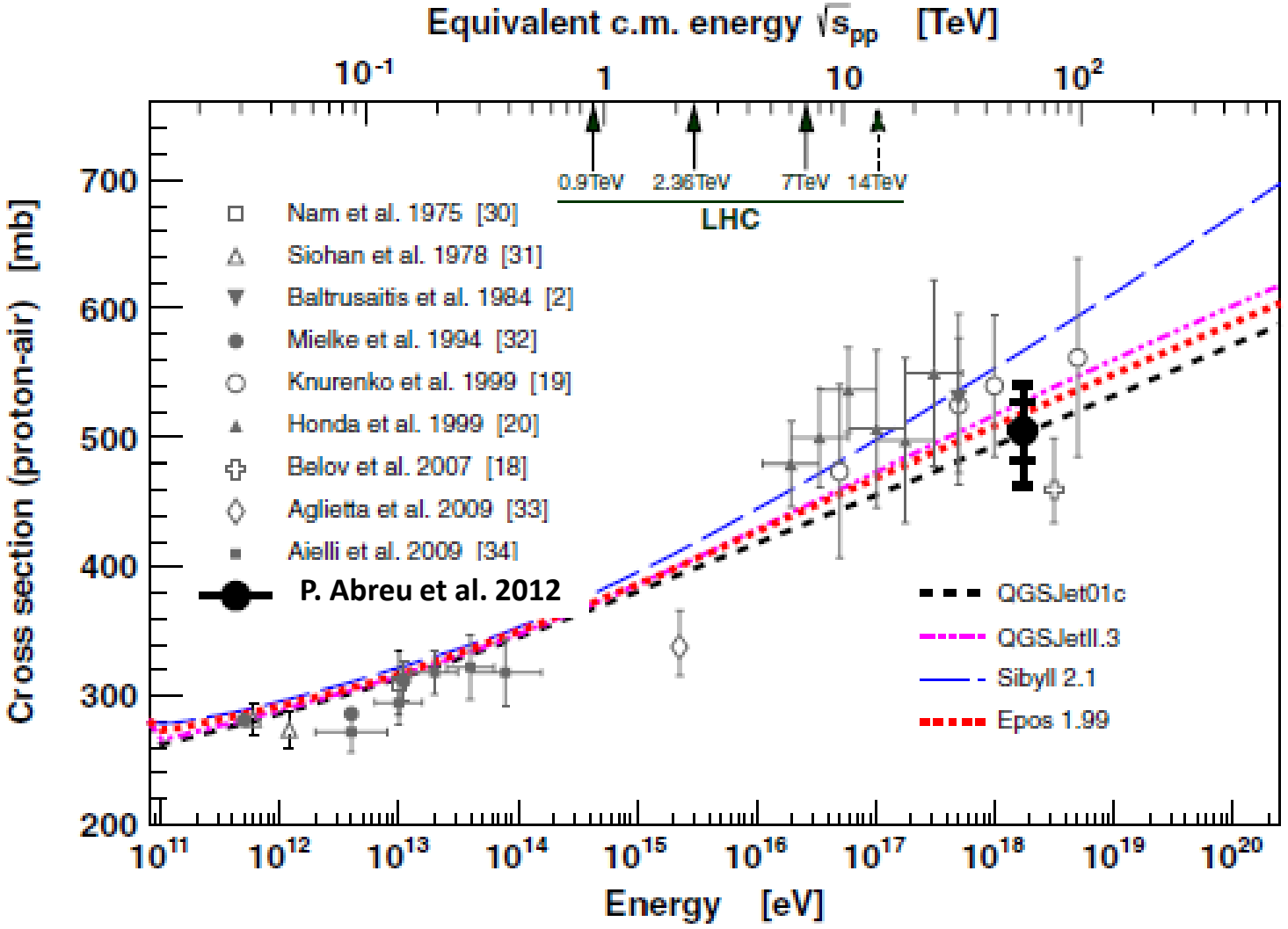

$^{+28}_{-36}$ mb .

$= 92^{+9}_{-11}$ mb

Pierre Auger Collaboration data from:
P. Abreu et al. [Pierre Auger Collaboration], Phys. Rev. Lett. 109 (2012) 062002 [arXiv:1208.1520 [hep-ex]].

Results:

Recently,
cross sect

There wa

From our

$\sigma_{p+N}^{prod,\ h}$

and

$\sigma_{p+N}^{prod,\ G}$

what dete
and is in c

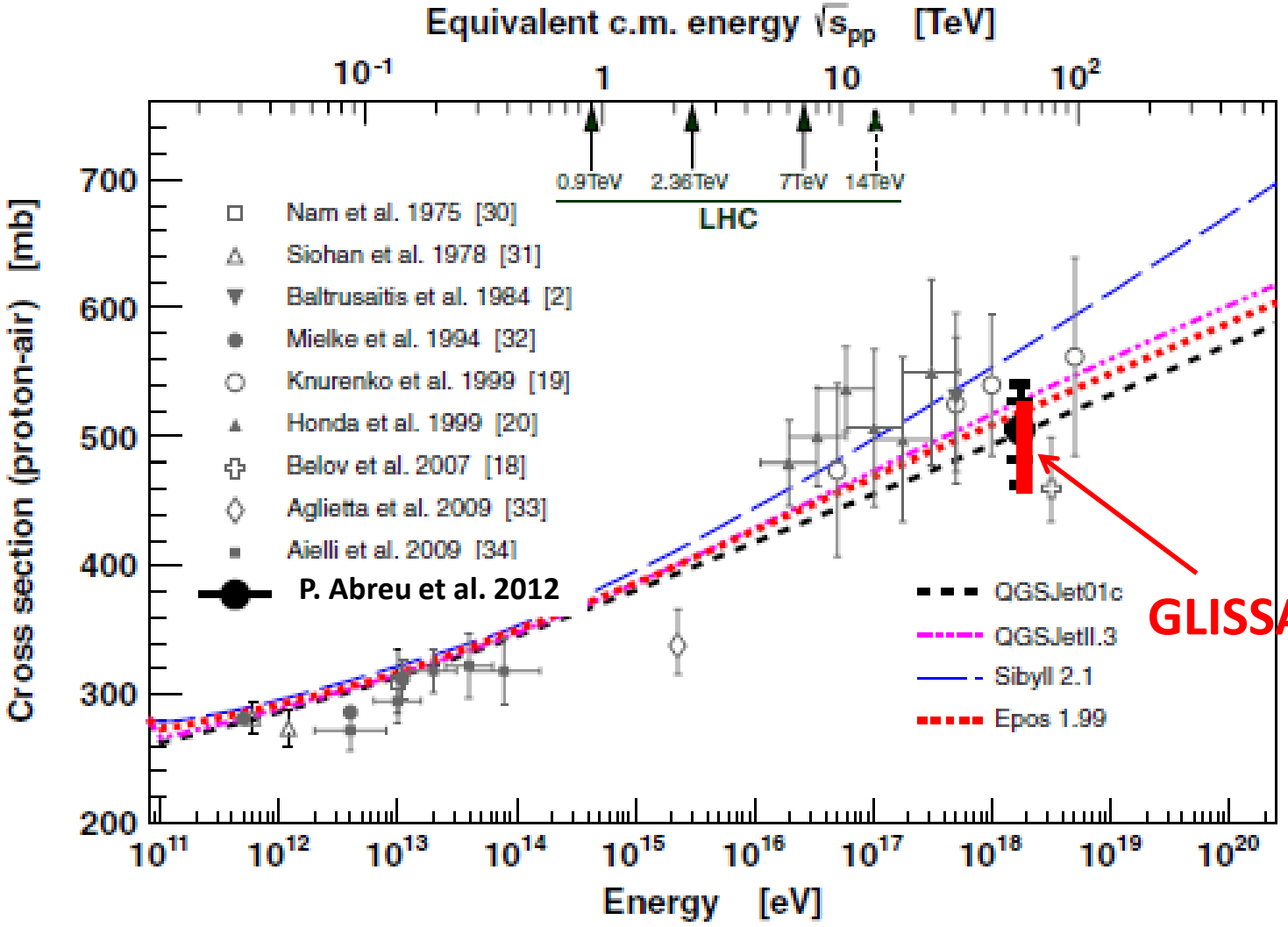

$^{+28}_{-36}$ mb .

$= 92^{+9}_{-11}$ mb

Pierre Auger Collaboration data from:
P. Abreu et al. [Pierre Auger Collaboration], Phys. Rev. Lett. 109 (2012) 062002 [arXiv:1208.1520 [hep-ex]].

Results:
inelastic nucleon-nucleon cross section

From the other side, with the use of Eqs. (*) and (**) it is possible to estimate the range of σ^{inel} at $\sqrt{s} = 57\ \mathrm{TeV}$.

We recovered the Pierre Auger Collaboration $\sigma_{p+N}^{prod} = 505\ \mathrm{mb}$ at

$\sigma^{inel} = 87\ \mathrm{mb}$ (Gaussian approximation)

and

$\sigma^{inel} = 116\ \mathrm{mb}$ (hard-sphere approximation).

Pierre Auger Collaboration data from:
P. Abreu et al. [Pierre Auger Collaboration], Phys. Rev. Lett. 109 (2012) 062002 [arXiv:1208.1520 [hep-ex]].

Results:

inelastic nucleon-nucleon cross section

From the oth
the range of

We recovere

$\sigma^{inel} = 87$

and

$\sigma^{inel} = 11($

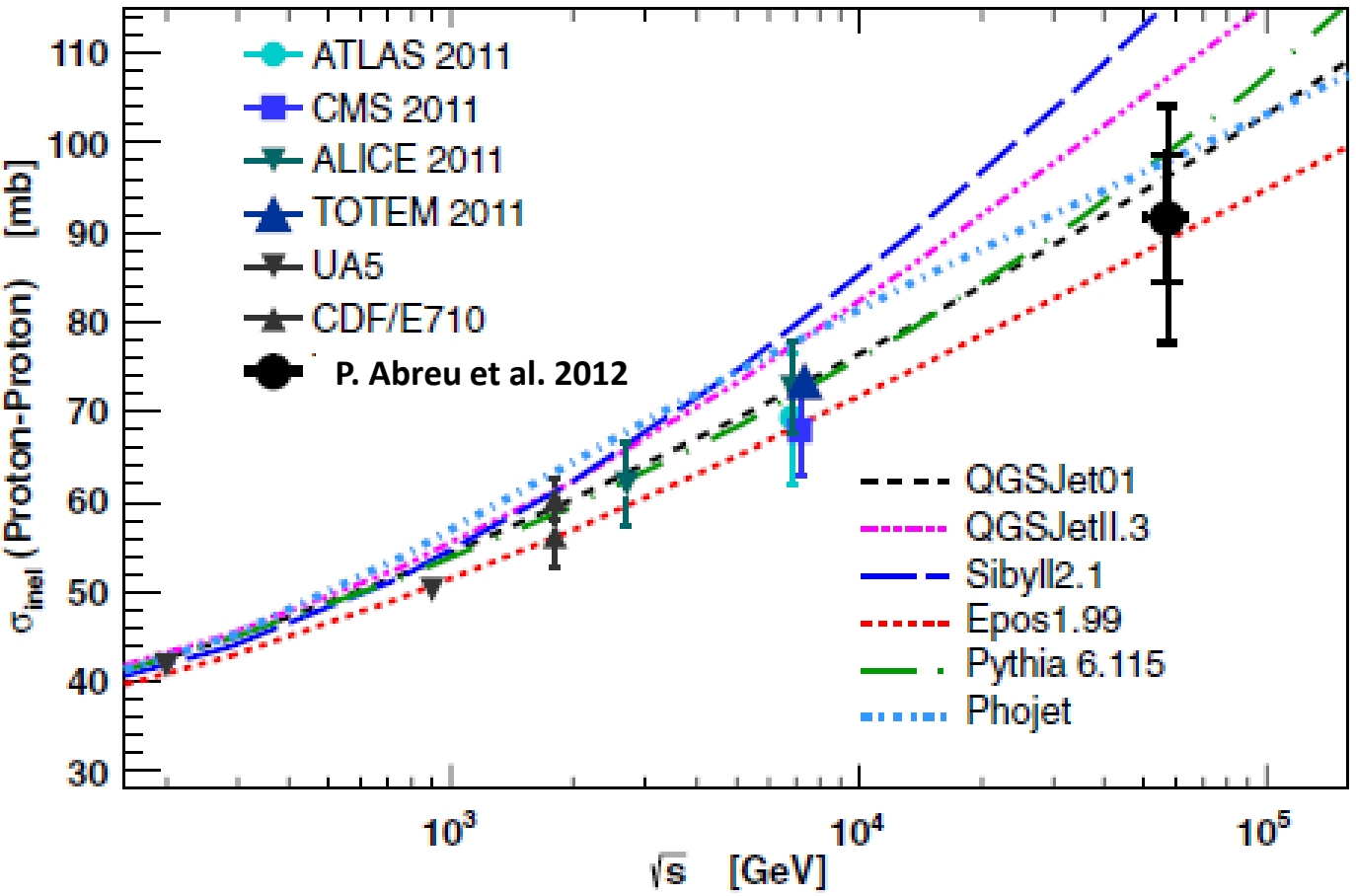

Pierre Auger Collaboration data from:
P. Abreu et al. [Pierre Auger Collaboration], Phys. Rev. Lett. 109 (2012) 062002 [arXiv:1208.1520 [hep-ex]].

Results:

inelastic nucleon-nucleon cross section

From the oth
the range of

We recovere

$\sigma^{inel} = 87$

and

$\sigma^{inel} = 11($

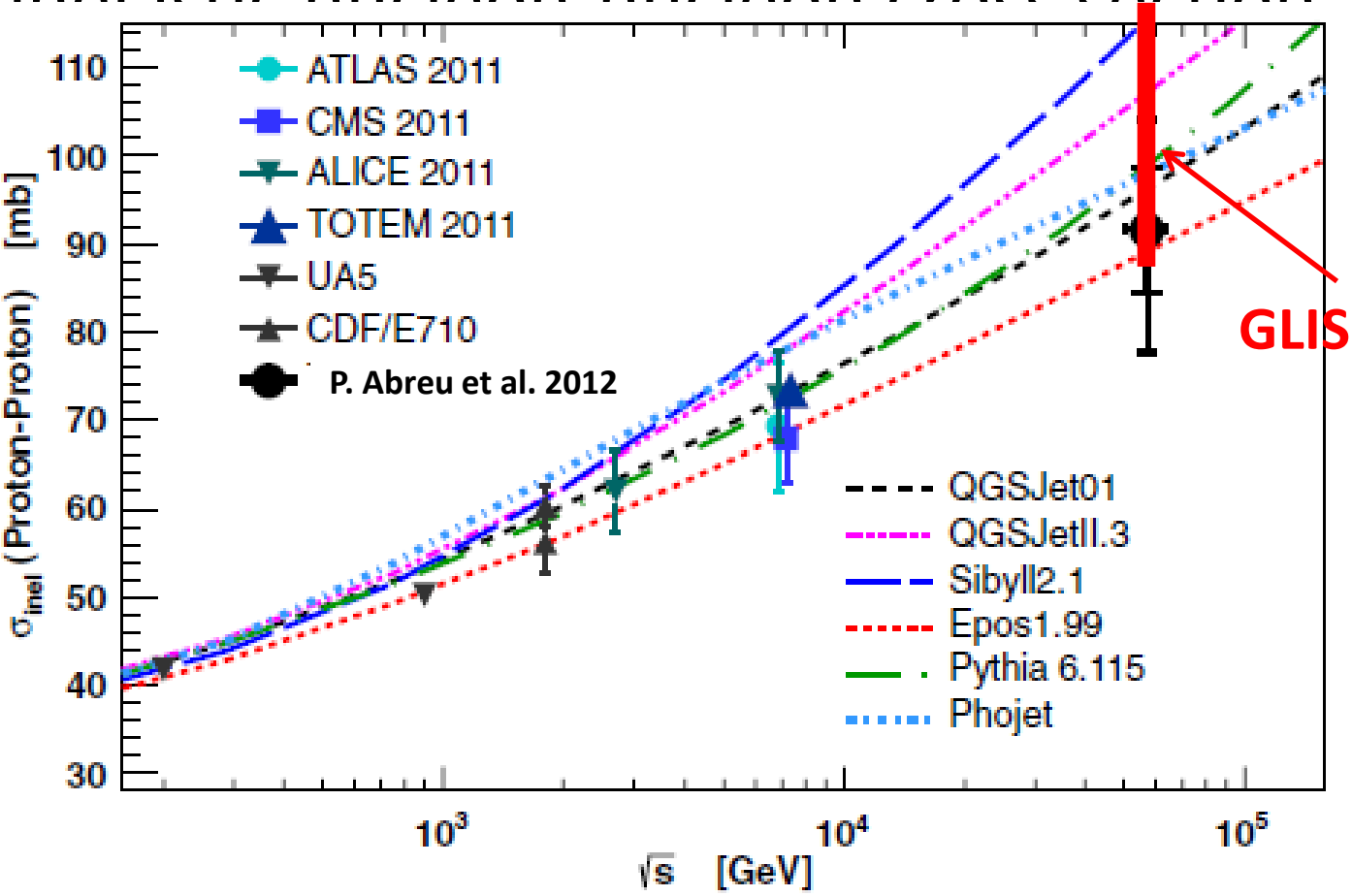

GLISSANDO

Pierre Auger Collaboration data from:
P. Abreu et al. [Pierre Auger Collaboration], Phys. Rev. Lett. 109 (2012) 062002 [arXiv:1208.1520 [hep-ex]].

Results:

inelastic nucleon-nucleon cross section

From the oth
the range of

We recovere

$\sigma^{inel} = 87$

and

$\sigma^{inel} = 11($

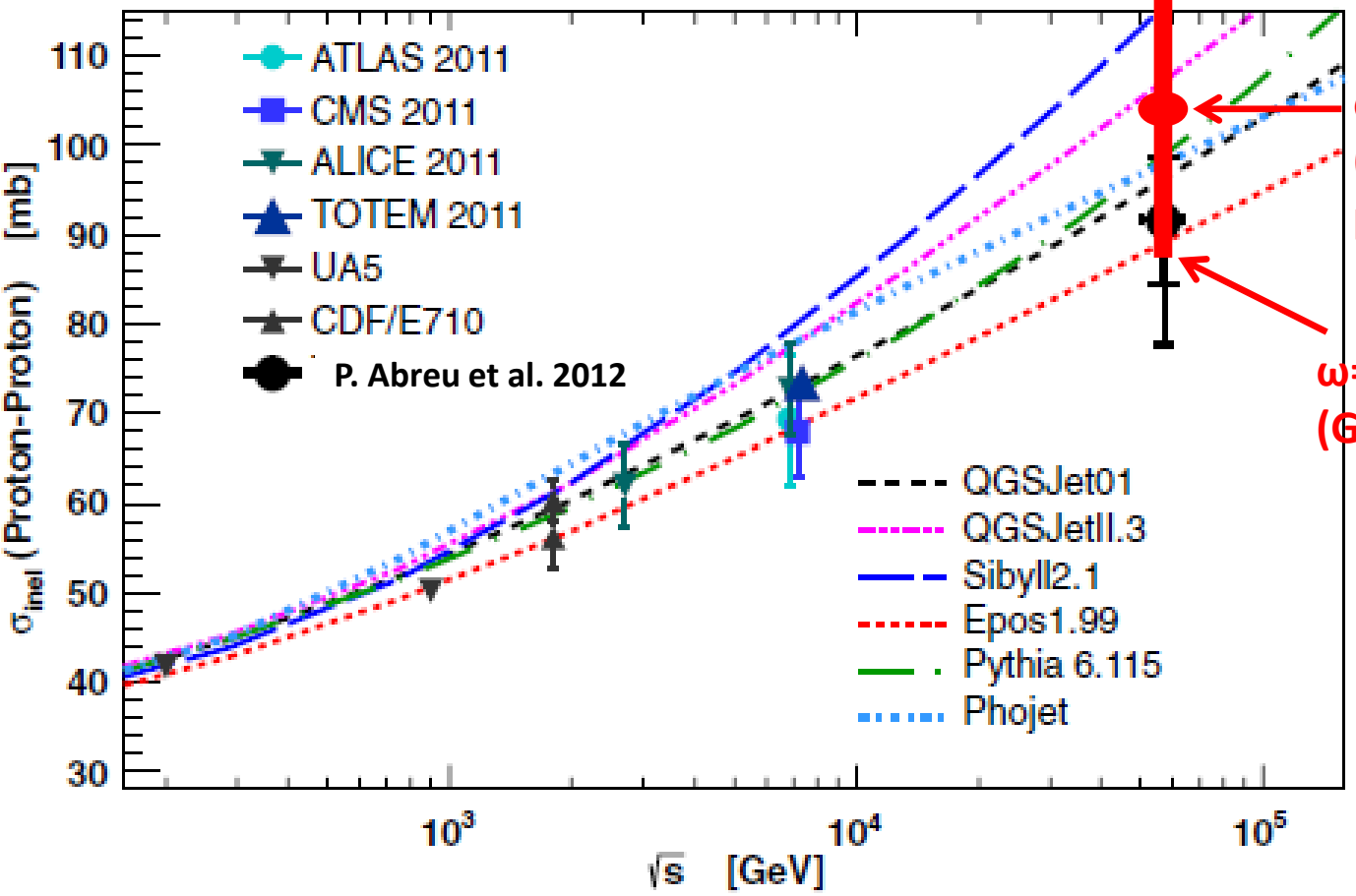

ω=0
(hard-sphere)

ω=0.4
(gamma,
preferred)

ω=1
(Gaussian)

Pierre Auger Collaboration data from:
P. Abreu et al. [Pierre Auger Collaboration], Phys. Rev. Lett. 109 (2012) 062002 [arXiv:1208.1520 [hep-ex]].

Conclusions (I)

The mean number of target participants as a function of atomic mass of target nucleus was plotted and discussed. A simple power-law fit with the exponent around $1/3$ was found to properly describe the above dependence for SPS as well as LHC energies. The value of this exponent slightly increases with the increasing energy of collision.

Conclusions (I)

The mean number of target participants as a function of atomic mass of target nucleus was plotted and discussed. A simple power-law fit with the exponent around $1/3$ was found to properly describe the above dependence for SPS as well as LHC energies. The value of this exponent slightly increases with the increasing energy of collision.

Fluctuations of target participants, described by the scaled variance of the distribution of the number of target participants, were plotted as a function of target nucleus mass and collision centre-of-mass energy. An influence of nucleon-nucleon wounding profile on scaled variance was discussed.

Conclusions (I)

The mean number of target participants as a function of atomic mass of target nucleus was plotted and discussed. A simple power-law fit with the exponent around $1/3$ was found to properly describe the above dependence for SPS as well as LHC energies. The value of this exponent slightly increases with the increasing energy of collision.

Fluctuations of target participants, described by the scaled variance of the distribution of the number of target participants, were plotted as a function of target nucleus mass and collision centre-of-mass energy. An influence of nucleon-nucleon wounding profile on scaled variance was discussed.

Production cross section as a function of target mass was estimated and fitted by power-law formula with the exponent around $2/3$. The value of the exponent slightly decreases with the increasing energy of collision.

Conclusions (I)

The mean number of target participants as a function of atomic mass of target nucleus was plotted and discussed. A simple power-law fit with the exponent around $1/3$ was found to properly describe the above dependence for SPS as well as LHC energies. The value of this exponent slightly increases with the increasing energy of collision.

Fluctuations of target participants, described by the scaled variance of the distribution of the number of target participants, were plotted as a function of target nucleus mass and collision centre-of-mass energy. An influence of nucleon-nucleon wounding profile on scaled variance was discussed.

Production cross section as a function of target mass was estimated and fitted by power-law formula with the exponent around $2/3$. The value of the exponent slightly decreases with the increasing energy of collision.

For $p + {}^{14}N$ interactions, the production cross section, σ_{p+N}^{prod} at $\sqrt{s} = 7\ \mathrm{TeV}$ was estimated to be equal $\sigma_{p+N}^{prod} = 394.3^{+5.1}_{-3.3}\ \mathrm{mb}$. Additionally, the dependence on total inelastic proton–proton cross section was found and described by power-law functions for hard-sphere and Gaussian nucleon–nucleon wounding profiles.

Conclusions (I)

The mean number of target participants as a function of atomic mass of target nucleus was plotted and discussed. A simple power-law fit with the exponent around $1/3$ was found to properly describe the above dependence for SPS as well as LHC energies. The value of this exponent slightly increases with the increasing energy of collision.

Fluctuations of target participants, described by the scaled variance of the distribution of the number of target participants, were plotted as a function of target nucleus mass and collision centre-of-mass energy. An influence of nucleon-nucleon wounding profile on scaled variance was discussed.

Production cross section as a function of target mass was estimated and fitted by power-law formula with the exponent around $2/3$. The value of the exponent slightly decreases with the increasing energy of collision.

For $p + {}^{14}N$ interactions, the production cross section, σ_{p+N}^{prod} at $\sqrt{s} = 7\ \mathrm{TeV}$ was estimated to be equal $\sigma_{p+N}^{prod} = 394.3^{+5.1}_{-3.3}\ \mathrm{mb}$. Additionally, the dependence on total inelastic proton–proton cross section was found and described by power-law functions for hard-sphere and Gaussian nucleon–nucleon wounding profiles.

The range of production $p + {}^{14}N$ cross section $\left(\sigma_{p+N}^{prod} \in (446, 525)\ \mathrm{mb}\right)$ as well as the range of total inelastic proton–proton cross section $\left(\sigma^{inel} \in (87, 116)\ \mathrm{mb}\right)$ at $\sqrt{s} = 57\ \mathrm{TeV}$ was estimated.

Conclusions (II)

- We hope that with its flexibility and simplicity GLISSANDO will become a useful tool for the heavy-ion community.
- The open-source nature of the code allows for check-ups additions and improvements.
- We have provided examples of numerous applications: determination of A+B cross-section and centrality classes, analysis of eccentricities both in the fixed- and variable-axes frame, event-by-event fluctuations, correlation of various quantities.
- Program is obtainable from: http://www.ujk.edu.pl/homepages/mryb/GLISSANDO/
- We can assist anyone interested in running the code or tayloring it to his/her needs (for the price of one citation!)

Additional slides

Original relevant features of the code

Possibility of superimposing a distribution of weights over the distribution of individual sources, reflecting the fact that the elementary collisions may result in the deposition of a varying amount of the entropy/energy.

The realistic Gaussian wounding profile for the NN collisions
(M. Rybczynski and W. Broniowski, Phys.Rev. C84, 064913).

The built-in analysis of the shape fluctuations
(PHOBOS, S. Manly et al., Nucl. Phys. A774, 523; S.A. Voloshin, nucl-th/0606022;
W. Broniowski, P. Bozek and M. Rybczynski, Phys.Rev. C76, 054905).

Evaluation and storage of the two-dimensional density profiles to be used „off-line" in other analyses, such the event-by-event initial condition for hydrodynamics, jet quenching, etc.

The code can be directly used for proton-nucleus and deuteron-nucleus collisions.
The Hulthen distribution is used to describe the NN separation in the deuteron.

The code uses the ROOT libraries and data structures.

New version has more features

Parameterization of shape of all nuclei, including light nuclei. This will be useful in applications to the NA61 experiment, where the mass-number scan will be carried out.

Inclusion of the deformation of the colliding nuclei. In particular, the deformation effects are relevant for the collisions involving the Au and U nuclei
(M. Rybczynski, W. Broniowski and G. Stefanek, Phys. Rev. C 87, 0044908).

Possiblity of using correlated distributions of nucleons in nuclei, which may be read in from external files prepared with other codes.
Certainly, two-body correlations are important, as they influence the fluctuations
(W. Broniowski and M. Rybczynski, Phys.Rev. C81, 064909).

Possibility of overlaying distributions of the produced particles which depend on the space-time rapidity. This feature extends the model into a fully 3+1 dimensional tool.

Inclusion of the core-corona efect
(C. Hohne, F. Puhlhofer and R. Stock, Phys. Lett. B640, 96).

The structure of the C++ code has been simplified.

A doxygen-generated reference manual is available for those, who wish to alter the code for their needs.

General features of GLISSANDO 2

The program generates inter alia the variable-axes (participant) two- and three-dimensional profiles of the density of sources in the transverse plane and their Fourier components.

Pb+Pb@5.5 TeV/n, Core-corona distributions

core - collided more than once
corona- collided once

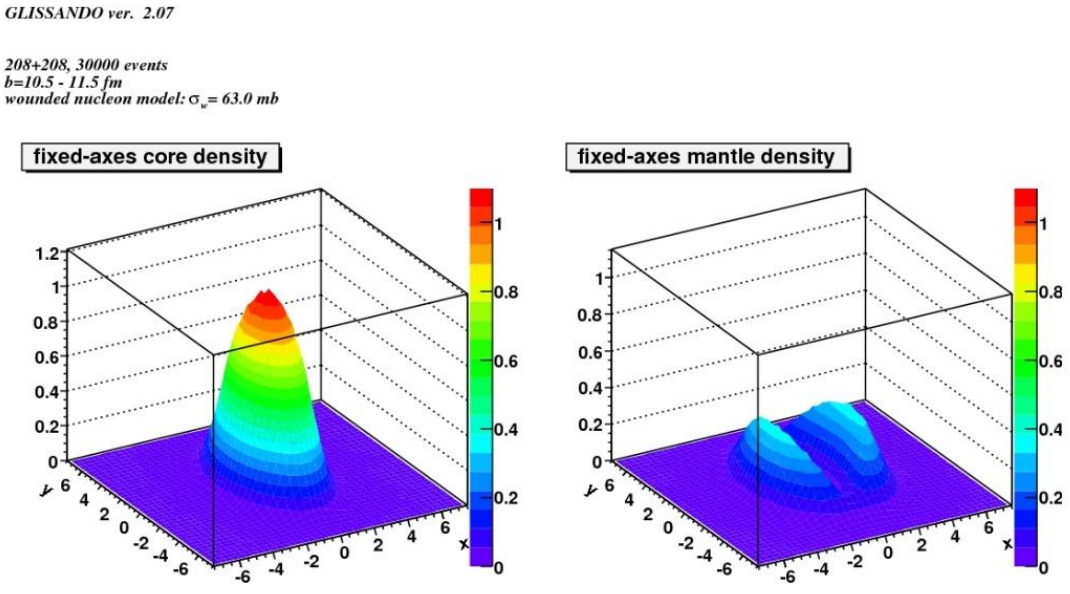

Details in:
P. Bożek, Acta Phys.Polon. B36, 3071
K. Werner, Phys. Rev. Lett. 98, 152301

These profiles can be used in further analyses of physical phenomena, such as the jet quenching, event-by-event hydrodynamics, or analysis of the elliptic flow and its fluctuations.

General features of GLISSANDO 2

Characteristics of the event (multiplicities, eccentricities, Fourier coefficients, etc.) are evaluated and stored in a file for further off-line studies.
A number of scripts is provided for that purpose.

GLISSANDO ver. 2.07
(nuclear distributions from files)
208+208, 1000000 events
b=0.0 - 24.0 fm
mixed model: σ_w= 63.0 mb, σ_{bin}=63.0 mb, α=0.200

Pb+Pb@5.5 TeV/n

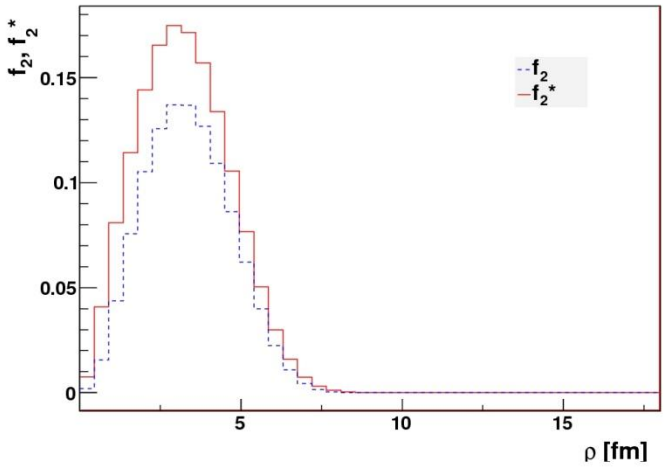

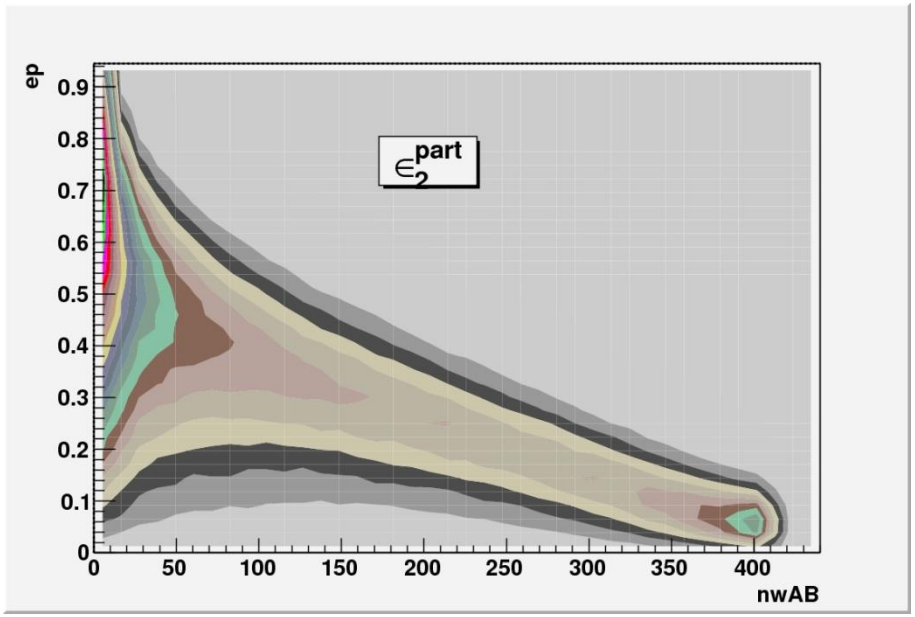

f_2 - radial profile of the second Fourier harmonic - fixed axes
f_2* - radial profile of the second Fourier harmonic - variable axes (participant geometry)
(can be used to emulate initial conditions for event-by-event hydro)

Other possibilities

- Possibility of overlaying rapidity distribution over the distribution of sources
- Tilted boundary condition

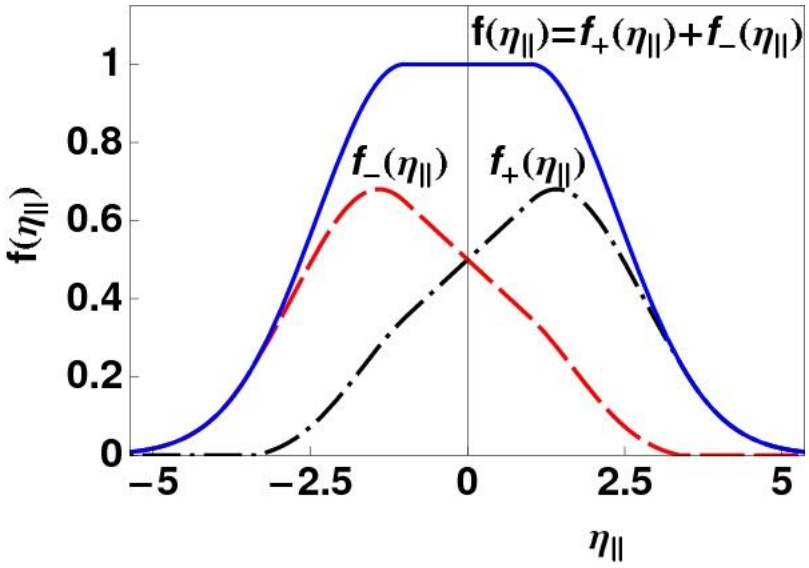

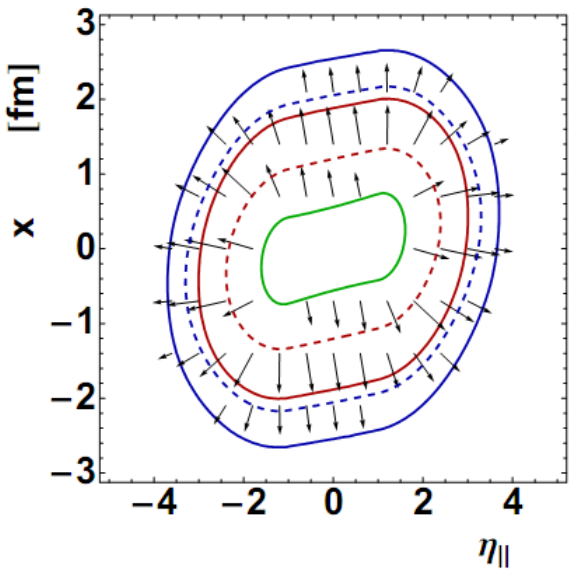

P. Bożek, and I. Wyskiel, Phys. Rev. C81, 054902
explains for the first time the directed flow v_1 in the hydro approach!

Other possibilities

- Triangular flow

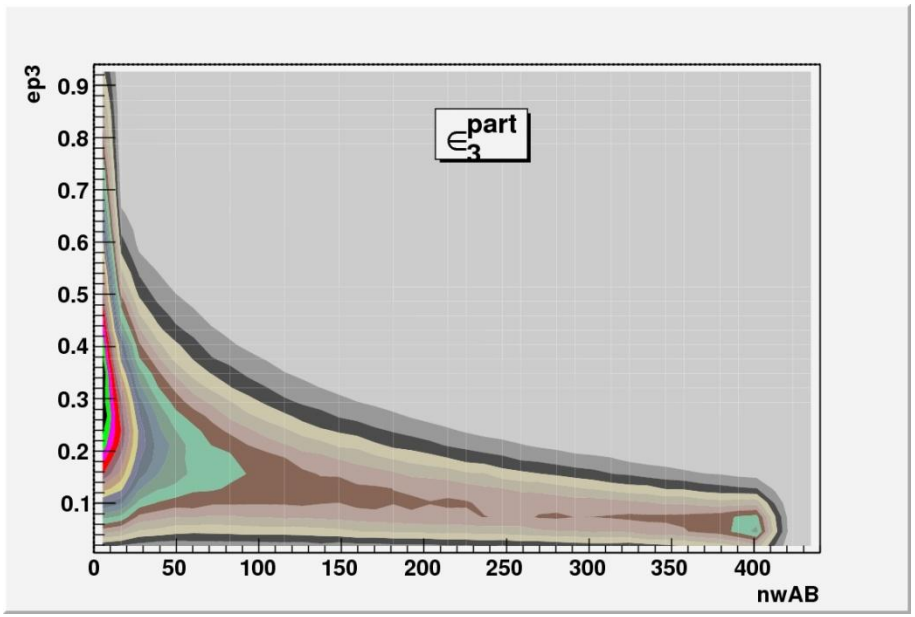

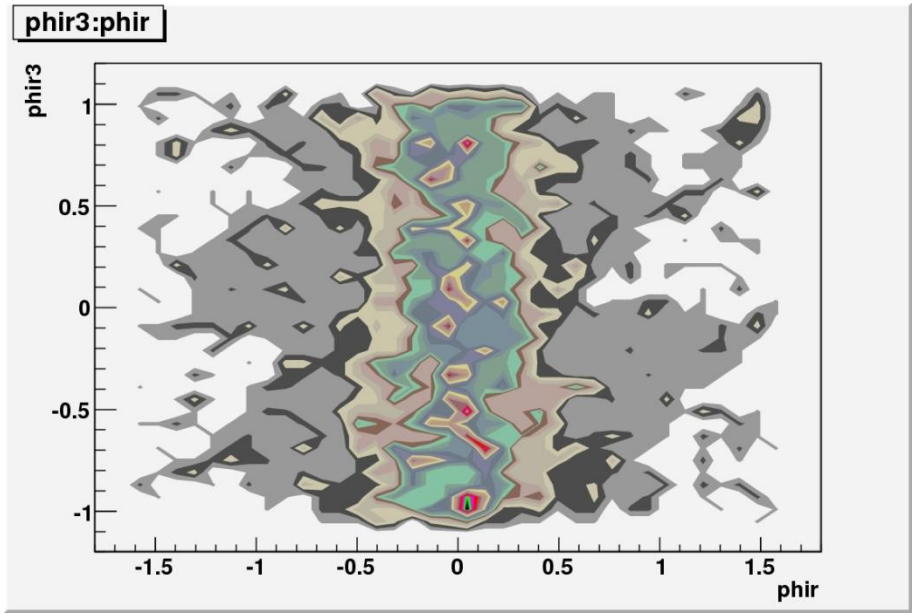

- ε_3^{part} - the triangular deformation coefficient
- lack of correlation between the axes which maximize the second and third Fourier moment

See: Alver and Roland, Phys. Rev. C81, 054905
Alver et al., arXiv:1007.5469